

Properties of sodium-driven bacterial flagellar motor: A two-state model approach

Yunxin Zhang,

Shanghai Key Laboratory for Contemporary Applied Mathematics, Laboratory of Mathematics for Nonlinear Science, Centre for Computational Systems Biology, School of Mathematical Sciences, Fudan University, Shanghai 200433, China. E-mail: xyz@fudan.edu.cn

Abstract

Bacterial flagellar motor (BFM) is one of the ion-driven molecular machines, which drives the rotation of flagellar filaments and enable bacteria to swim in viscous solutions. Understanding its mechanism is one challenge in biophysics. Based on previous models and inspired by the idea used in description of motor proteins, in this study one two-state model is provided. Meanwhile, according to corresponding experimental data, mathematical relationship between BFM membrane voltage and pH value of the environment, and relationship between internal and external sodium concentrations are given. Therefore, with model parameter values obtained by fitting theoretical results of torque-speed relation to recent experimental data, many biophysical properties of bacterial flagellar motor can be obtained for any pH values and any external sodium concentrations. Including the rotation speed, *stall torque* (i.e. the torque generated by BFM), rotation dispersion, and rotation randomness. In this study, the single-stator BFM will be firstly analyzed, and then properties of multiple-stator BFM are addressed briefly.

Author Summary

Based on previous models for BFM and the idea used in the modeling of motor protein kinesin, one two-state model is present to discuss biophysical properties of BFM. From this model torque-speed relationship, dispersion and randomness of single-stator BFM can be obtained for any pH values and any external sodium concentrations. Meanwhile properties of BFM with multiple stators are also discussed.

Introduction

Ion-motive force (IMF), which comprises electrical and chemical transmembrane potential, is essential for biophysical functioning of cells [1–4]. Two primary forms of IMF are *proton-motive force* (PMF) and *sodium-motive force* (SMF). Many cellular processes, including bacterial motility, ATP synthesis and active membrane transport, are driven by SMF [5–8]. Recently, molecular machines driven by IMF have been extensively studied both experimentally and theoretically. The studies in [9–12] found that, the energy efficiency of the F_1 part of F_0F_1 -ATP synthase, which transduces energy between chemical free energy and mechanical work, is almost 100%. In [13,14], coarse-grained models are employed to under the mechanism of F_1 -ATPase and F_0 -ATPase. Meanwhile, the catalytic power of F_1 -ATPase is detailed analyzed in [15], the structure and organization of the yeast F_0F_1 -ATP synthase are studied in [16], and the Na^+ , K^+ -ATPase in liposomal membrane are discussed in [17]. Finally, more theoretical studies can also be found in [18–32] for F_0 -ATPase or F_1 -ATPase, and in [33–41] for transmembrane motion of ions.

One of the most important molecular machines driven by IMF is bacterial flagellar motor (BFM), which couples ion flow (H^+ or Na^+) to the rotation of extracellular helical flagellar filaments at hundreds of revolutions per second (Hz), and then propels many species of swimming bacteria [42]. Using the transmembrane electrochemical H^+ (or Na^+) gradient to power rotation of the flagellar motor, free-swimming bacteria can propel their cell body at a speed of 15-100 mm/s, or up to 100 cell body lengths/s [6,43]. The BFM has one rotor and multiple stators in a circular ring-like structure ≈ 45 nm in diameter [44]. The stators are attached to the rigid peptidoglycan cell wall and the spinning of the rotor drives the flagellar filament through a short hook. In *E. coli*, the rotor is composed of a ring of ~ 26 FliG proteins and each stator has 4 copies of proteins MotA and 2 copies of proteins MotB, forming 2 proton-conducting transmembrane channels [45,46]. The stator can deliver torque to the rotor by converting the free energy of ion flow across the cytoplasmic membrane.

To understand the biophysical properties and torque-generating mechanism of BFM, many experiments have been done to measure revolution speed under varying torque [47–55]. Meanwhile, various biophysical and biochemical models have also been constructed to try to understand the basic principle of BFM [45–47, 56–59]. However, so far most of the previous studies mainly focused on the torque-speed relationship, except in [54, 58] where effect of pH value on torque-speed relation is discussed, and in [59] where effects of pH value and membrane potential are analyzed theoretically, and in [45, 48, 49, 57] where

the effect of temperature (or noise) on the speed of BFM is addressed, and in [50, 51] where the effect of Na^+ concentration is studied experimentally.

In recent study of Lo *et al* [60], one three-state model was presented to describe the torque-speed relationship of one-stator BFM under various pH values and various external sodium concentrations. Their model can fit experimental data well, in which one of the basic parameters is the electrical energy $U = qV_m$, with V_m the membrane voltage. Experimental data shows that membrane voltage V_m depends on surrounding solution (see [60] and references there in). This study found that, the value of V_m depends only on the pH value of the solution, and is independent of the external sodium concentration $[\text{Na}]_{ex}$ [see Fig. 1(a)]. Moreover, V_m changes almost linearly with pH value,

$$V_m = -28.04\text{pH} + 57.88, \quad (1)$$

with voltage in millivolt unit (mV). On the other hand, besides pH value and external sodium concentration $[\text{Na}]_{ex}$, the value of internal sodium concentration $[\text{Na}]_{in}$ is also needed to obtain the *sodium-motive force*, since it comprises electrical transmembrane potential V_m and chemical transmembrane potential $\Delta\mu/q$ and is defined as

$$\text{SMF} = V_m + \frac{\Delta\mu}{q} = V_m + \frac{k_B T}{q} \ln \left(\frac{[\text{Na}]_{in}}{[\text{Na}]_{ex}} \right), \quad (2)$$

where $q = 1.602 \times 10^{-19}$ coulomb (C) is the charge of sodium ion, k_B is the Boltzmann constant, and T is the absolute temperature. Further analysis about the experimental data shows that the internal sodium concentration $[\text{Na}]_{in}$ can be well approximated by [see Fig. 1(b)]

$$[\text{Na}]_{in} = 9.013[\text{Na}]_{ex}/(1.318 + [\text{Na}]_{ex}). \quad (3)$$

In fact, this relation is similar as the one used to approximate ADP concentration by ATP concentration in the study of motor protein kinesin [61].

Different with the three-state model used in [60], in this study one simple two-state model will be presented to describe the rotation of one-stator BFM. With relationships (1) and (3), properties for one-stator BFM under any pH values and external sodium concentrations will be obtained, such as the torque-speed relationship, the *stall torque* Γ_s (i.e. the torque under which the rotation speed V of BFM vanishes), dispersion D and randomness r . The results show that, both rotation speed V and *stall*

torque Γ_s increase with pH value and sodium concentration $[\text{Na}]_{ex}$. Under high pH value and sodium concentration $[\text{Na}]_{ex}$, the rotation of one-stator BFM can be regarded as one Possion process, i.e. process with only one internal state. Meanwhile, in this study properties of BFM with multiple stators will also be discussed.

Results

In previous studies, four-state model is usually used to describe the rotation of BFM [50, 53, 54]. However, such model has 25 free model parameters which makes it difficult to fit corresponding data, and special Monte Carlo search strategy should be given to overcome this difficulty [60]. For simplicity, and inspired by the corresponding idea used in the modeling of motor proteins [61, 62], one two-state model is presented in this study. Compared with the four-state model, this two-stator model has only 10 free parameters, which is even less than that of the reduced three-state model as used in [60]. Moreover, by this two-state model, it is much convenient to do further theoretical analysis to know more biophysical properties about the rotation of BFM. For example, the dispersion D and randomness $r = 2D/V\varphi$ can be easily obtained. At the same time, by the relationship between membrane voltage V_m and pH value as given in Eq. (1), and the relationship between internal sodium concentration $[\text{Na}]_{in}$ and external sodium concentration $[\text{Na}]_{ex}$ as given in Eq. (3), properties of BFM rotation can be obtained for any pH values and any external sodium concentrations (in the recent paper of Lo *et al* [60], only torque-speed relationships for pH=5, 5.5, 6, 6.5, 7, and external sodium concentration $[\text{Na}]_{ex}=1$ mM, 5 mM, 10 mM, 30 mM, 85 mM are provided, see also Fig. 3). The fitting results given in Fig. 3 show that, with appropriate parameter values (see TABLE 1), this two-state model can explain experimental data reasonably.

As mentioned previously, using formulations given in Eqs. (1) and (3), properties of BFM rotation can be obtained for any pH values and any external sodium concentrations $[\text{Na}]_{ex}$. The plots in Fig. 4 show that, under any external torques BFM rotation speed V increases monotonically with pH value and external sodium concentration $[\text{Na}]_{ex}$. For high concentration $[\text{Na}]_{ex}$ and pH values, V increases almost experimentally with pH value. Further calculations indicate that, with the increase of sodium concentration $[\text{Na}]_{ex}$, the rotation speed V will tend to one limit value. Since for high external concentration $[\text{Na}]_{ex}$, the internal concentration $[\text{Na}]_{in}$, and consequently the transition rate k_4 , is almost invariable [see Eq. (3)]. So the rotation speed as given in Eq. (6) satisfies $V \rightarrow k_3\varphi$.

The plots in Fig. 5 show that, the *stall torque* Γ_s , i.e. the torque which satisfies $V(\Gamma_s) = 0$, increases linearly with pH value and almost linearly with the logarithm of external sodium concentration $\ln[\text{Na}]_{ex}$, see also Eq. (7). So concentrations of proton and sodium ion not only have effect on rotation speed V , but also can change the maximum output work $W_{\max} = \Gamma_s \varphi$ [63, 64]. Further calculations show that other biophysical quantities, such as the maximum output power $P_{\max} = \max_{\Gamma} \Gamma V(\Gamma)$, and efficiency at maximum output power $\eta_{\max} = \Gamma_{\max}/\Gamma_s$, depend also on pH value and sodium concentration $[\text{Na}]_{ex}$ [65]. Where Γ_{\max} is the external torque under which the output power of BFM reaches its maximum P_{\max} .

Besides rotation speed V and *stall torque* Γ_s , the dispersion D of BFM rotation also increases with pH value and external sodium concentration $[\text{Na}]_{ex}$, see Fig. 6(a, b). Here dispersion D , also called *effective diffusion constant*, is defined by $D = 1/2 \lim_{t \rightarrow \infty} d[\langle \theta^2(t) \rangle - \langle \theta(t) \rangle^2]/dt$ [61, 66, 67]. However, with the increase of pH value and external sodium concentration $[\text{Na}]_{ex}$, the randomness $r = 2D/V\varphi$ decreases to 1 monotonically. Which means that, under high pH value and high sodium concentration $[\text{Na}]_{ex}$, the BFM rotation is just one Poisson process [68]. As discussed before, in such cases, the forward transition $1 \xrightarrow{k_1} 2$ is fast, and the rotation is mainly limited by the forward transition $2 \xrightarrow{k_3} 1$, see Fig. 2(b).

Since one BFM may include multiple stators, the external torque is then shared by all the working stators. So the *stall torque* of BFM with n stators should be n times of which of the single stator BFM, while the maximum rotation speeds (i.e. speeds without external torque) are the same [45, 47, 60], see Fig. 7. However, for a BFM with M stators, the M stators may not work all the time. In other words, some stators may be dissociated from the rotor of BFM. So they are in idle state, or their rotation have no effective contribution to the BFM rotation. Therefore, for multiple stator BFM, the torque-speed relationship may be different from the ones plotted in Fig. 7. Actually, the actual rotation speed is slightly lower than that plotted in Fig. 7 (figures not shown here). In the following, the properties of BFM with multiple stators will be discussed.

Three examples of probability p_n that there are n stators in working to rotate the BFM are given in Fig. 8(a) for a BFM with total $M = 8$ stators. Although most of stators are engaged in the rotation of BFM, some may in unbinding state, especially when the external torque is low. The plots in Fig. 8(b) show that the mean binding number $\langle n \rangle$ of stator increases slightly with the external torque Γ , but is always less than the total stator number M . This indicates that, the BFM can adjust itself with the external torque, if the torque is low some stators may in idle state to save energy. Meanwhile, the mean

binding number $\langle n \rangle$ increases with sodium concentration $[\text{Na}]_{ex}$ [see Fig. 8(c)]. Since with high sodium concentration $[\text{Na}]_{ex}$ the transition rates k_1, k_4 are high [see Fig. 2(b) and discussion below Eq. (5)], consequently stators are more likely to transfer to the binding state **2**. Finally, the mean binding number $\langle n \rangle$ decreases with the pH value, see Fig. 8(d).

As mentioned before, usually the mean rotation speed $\bar{V} = \sum_{n=1}^M p_n V_n$ of a BFM with M stators is lower than its maximum speed V_M [the BFM speed provided all the M stators are bound to the BFM rotor (see Fig. 7 for V_M)]. But the plots in Fig. 9(a,b,c) show that, similar as V_M , mean rotation speed \bar{V} also decreases with external torque Γ , and increases with sodium concentration $[\text{Na}]_{ex}$ and pH value [also experimentally for large $[\text{Na}]_{ex}$ and pH value, Fig. 4(a)]. This is because \bar{V} is merely the linear combination of V_n for $n = 1, 2, \dots, M$. As expected, the mean *stall torque* $\bar{\Gamma}_s$ increases with sodium concentration $[\text{Na}]_{ex}$ and pH value, and increased almost linearly with the total stator number M .

Discussion

In this study, the sodium driven bacterial flagellar motor (BFM) is theoretically analyzed. Based on the previous models used in [50, 53, 54, 60] and the idea used in [61, 62] for modeling description of motor protein kinesin, one simple two-state model is presented. Moreover, according to the experimental data collected in [60], relationship between membrane voltage and pH value, and relationship between internal and external sodium concentrations are explicitly given. So, by the two-state model, rotation speed of BFM can be obtained for any pH values and any external sodium concentrations. Meanwhile, in this study other biophysical properties of BFM are also studied, including *stall torque* (the torque under which the BFM rotation speed vanishes), dispersion and randomness. In reality, one BFM may have multiple stators. In this study, the properties of multiple-stator BFM are also addressed. Roughly speaking, the *stall torque* of a M -stator BFM is about M times of which of a single-stator BFM, and the external torque of BFM are usually shared by all the M stators. But under low torque, low sodium concentration and high pH value, some stators may be disassociated from BFM rotor and in idle state. Using this two-state model, other detailed biophysical properties can also be obtained, such as the maximum power and energy efficiency [64, 65, 69].

Materials and Methods

Two-state kinetic model for one-stator BFM

The two-state model used in this study, which is schematically depicted in Fig. 2(a), can be regarded as one combination of the three-state model presented in [60] for BFM and the two-state model given in [61] for motor protein kinesin. In brief, the rotation of stator can be regarded as motion of a particle in one tilted periodic potential $G(\theta)$ with period $\varphi = 2\pi/N$, i.e. periodic rotation with step-size φ . Where N is the number of ions passing through stator per revolution, and as in [60], $N = 37$ is used in this study. The same as in the modeling for motor protein kinesin [61], in each period potential $G(\theta)$ has two minima, corresponding to two transition states of stator when one ion passes through it. Or in other words, the stator has two states in each rotation step (with step-size φ), denoted by **1** and **2** respectively. Mathematically, the periodic rotation of stator can be simply described by the following Markov process (see also Fig. 2(b))

$$\cdots \xrightleftharpoons[k_4]{k_3} \textcircled{1} \xrightleftharpoons[k_2]{k_1} \textcircled{2} \xrightleftharpoons[k_4]{k_3} \textcircled{1} \xrightleftharpoons[k_2]{k_1} \cdots$$

During the forward rotation from state **1** to state **2**, stator should overcome energy barrier ΔG_1 , so the transition rate $k_1 \propto e^{-\Delta G_1/k_B T}$. Similarly, $k_i \propto e^{-\Delta G_i/k_B T}$ for $i = 2, 3, 4$. Where energy barrier ΔG_i depends on external torque Γ . Similar to the method as demonstrated in models of molecular motor and microtubule [61, 70, 71], this torque dependence can be approximated as follows

$$\Delta G_1 = \Delta G_1^0 + \epsilon_1 \Gamma \varphi, \quad \Delta G_2 = \Delta G_2^0 - \epsilon_2 \Gamma \varphi, \quad \Delta G_3 = \Delta G_3^0 + \epsilon_3 \Gamma \varphi, \quad \Delta G_4 = \Delta G_4^0 - \epsilon_4 \Gamma \varphi. \quad (4)$$

Where ΔG_i^0 (for $i = 1, 2, 3, 4$) are intrinsic energy barriers, i.e. energy barriers when external torque Γ vanishes. Parameters ϵ_i are *load distribution factors* which satisfy normalization condition $\sum_{i=1}^4 \epsilon_i = 1$. The electrical energy U released by one ion when passing through stator can be decomposed into two parts, $U = U_1 + U_2 := (\Delta G_2^0 - \Delta G_1^0) + (\Delta G_4^0 - \Delta G_3^0)$, with U_1 the energy released during forward transition $\mathbf{1} \xrightarrow{k_1} \mathbf{2}$, and U_2 the energy released during forward transition $\mathbf{2} \xrightarrow{k_3} \mathbf{1}$. Based on the above analysis, in the

two-state kinetic model, transition rates k_i (see Fig. 2(b)) can be obtained by the following formulations,

$$k_1 = k_1^0 e^{(\epsilon'_1 U - \epsilon_1 \Gamma \varphi)/k_B T}, \quad k_2 = k_2^0 e^{(-\epsilon'_2 U + \epsilon_2 \Gamma \varphi)/k_B T}, \quad k_3 = k_3^0 e^{(\epsilon'_3 U - \epsilon_3 \Gamma \varphi)/k_B T}, \quad k_4 = k_4^0 e^{(-\epsilon'_4 U + \epsilon_4 \Gamma \varphi)/k_B T}. \quad (5)$$

Where ϵ'_i are also *distribution factors* which satisfy $(\epsilon'_1 + \epsilon'_2) = U_1/U$, and $(\epsilon'_3 + \epsilon'_4) = U_2/U$. Energies $\epsilon'_1 U, \epsilon'_3 U$ are the parts to accelerate forward transitions $\mathbf{1} \xrightarrow{k_1} \mathbf{2}$ and $\mathbf{2} \xrightarrow{k_3} \mathbf{1}$ respectively. While $\epsilon'_2 U, \epsilon'_4 U$ are energies to reduce backward transitions $\mathbf{1} \xleftarrow{k_2} \mathbf{2}$ and $\mathbf{2} \xleftarrow{k_4} \mathbf{1}$ respectively.

Obviously, large electrical energy U and low external torque Γ will result in high forward transition rates k_1 and k_3 , but result in low backward transition rates k_2 and k_4 , and consequently will lead to high rotation speed. Similar as in [60], rates k_1^0, k_4^0 depend on external and internal sodium concentrations $[\text{Na}]_{ex}$ and $[\text{Na}]_{in}$ respectively. For simplicity, this study assumed that $k_1^0 = \hat{k}_1^0 [\text{Na}]_{ex}$, and $k_4^0 = \hat{k}_4^0 [\text{Na}]_{in}$ [61, 62]. As mentioned previously, electrical energy U can be obtained by $U = qV_m$, with membrane voltage V_m satisfying the formulation in Eq. (1).

Given the transition rates k_1, k_2, k_3, k_4 (see Fig. 2(b)), the mean rotation speed V and dispersion D of BFM can be easily obtained (see [63, 66, 67])

$$V = \frac{(k_1 k_3 - k_2 k_4) \varphi}{k_1 + k_2 + k_3 + k_4}, \quad D = \frac{\frac{1}{2}(k_1 k_3 + k_2 k_4) \varphi^2 - V^2}{k_1 + k_2 + k_3 + k_4}. \quad (6)$$

From the above formulation of rotation speed V , the *stall torque* Γ_s , i.e. the torque under which the rotation speed V vanishes, can be obtained as follows,

$$\Gamma_s = \frac{U}{\varphi} + \frac{k_B T}{\varphi} \ln \left(\frac{k_1^0 k_3^0}{k_2^0 k_4^0} \right) = \frac{NqV_m}{2\pi} + \frac{Nk_B T}{2\pi} \ln \left[\frac{(1.318 + [\text{Na}]_{ex}) \hat{k}_1^0 k_3^0}{9.013 k_2^0 \hat{k}_4^0} \right]. \quad (7)$$

Meanwhile, the randomness of BFM rotation can be obtained by $r = 2D/V\varphi$. By fitting to data about the torque-speed relationship presented in [60], the model parameters used in this study are listed in TABLE 1.

Analysis for multiple-stator BFM

Generally, one BFM may include multiple stators. Let $\lambda_k(\Gamma), \mu_k(\Gamma)$ be the binding and unbinding rates of stators to and from BFM rotor, provided that there are k binding stators. One can easily get

the the following equations

$$\begin{aligned}
\frac{dp_0}{dt} &= \mu_1(\Gamma)p_1 - n\lambda_0(\Gamma)p_0, \\
\frac{dp_n}{dt} &= [(M-n+1)\lambda_{n-1}(\Gamma)p_{n-1} + (n+1)\mu_{n+1}(\Gamma)p_{n+1}] - [(M-n)\lambda_n(\Gamma) + n\mu_n(\Gamma)]p_n, \quad \text{for } 1 \leq n \leq M-1, \\
\frac{dp_M}{dt} &= \lambda_{M-1}(\Gamma)p_{M-1} - M\mu_M(\Gamma)p_M.
\end{aligned} \tag{8}$$

Where p_n is the probability that BFM rotor is bound by n stators, M is the total number of stators, and

$$\lambda_n(\Gamma) = k_1(\Gamma/(n+1)) + k_4(\Gamma/(n+1)), \quad \mu_n(\Gamma) = k_2(\Gamma/n) + k_3(\Gamma/n). \tag{9}$$

Here, binding/unbinding of one stator to/from BFM rotor means that this stator will/won't be engaged in BFM rotation. This study assumes that all binding stators share external torque Γ equally (see Eq. (9)), which is similar as the one used for describing cargo motion in cells by multiple motor proteins [72–74]. The expressions given in Eq. (9) based on the assumption that, one stator in state **2** means it is bound to the BFM rotor, and conversely one stator in state **1** means it is unbound from the BFM rotor.

At steady state, one can show that [66, 70]

$$p_n = \left[\prod_{i=1}^n \left(\frac{u_{i-1}}{w_i} \right) \right] p_0, \quad \text{for } 1 \leq n \leq M, \tag{10}$$

where $u_n = (M-n)\lambda_n$, $w_n = n\mu_n$, and p_0 can be obtained by the normalization condition,

$$p_0 = \frac{1}{1 + \sum_{n=1}^M \left[\prod_{i=1}^n \left(\frac{u_{i-1}}{w_i} \right) \right]}. \tag{11}$$

From probability p_n , the mean binding number of stator can be obtained by $\langle n \rangle = \sum_{k=1}^M np_n$, and the mean rotation speed of BFM can be obtained by $\bar{V} = \sum_{k=1}^M p_n V_n$, where V_n is the rotation speed if there are n stators which are bound to the BFM rotor. The mean *stall torque* $\bar{\Gamma}_s$ is obtained by $\bar{V}(\bar{\Gamma}_s) = 0$.

Acknowledgments

This study was supported by the Natural Science Foundation of China (Grant No. 11271083), and the National Basic Research Program of China (National “973” program, project No. 2011CBA00804).

References

1. Hille B (2001) Ionic Channels of Excitable Membranes. 3rd ed. (Sinauer Associates, Sunderland, MA).
2. Bray D (2001) Cell movements: from molecules to motility, 2nd Edn. Garland, New York.
3. Howard J (2001) Mechanics of Motor Proteins and the Cytoskeleton. Sinauer Associates and Sunderland, MA.
4. Schliwa M (2003) Molecular Motors. Wiley-Vch, Weinheim.
5. Shultis DD, Purdy MD, Banchs CN, Wiener MC (2006) Outer membrane active transport: Structure of the BtuB:TonB complex. *Science* 312: 1396-1399.
6. Sowa Y, Berry RM (2008) Bacterial flagellar motor. *Q Rev Biophys* 41: 103-132.
7. Okuno D, Iino R, Noji H (2008) Rotation and structure of F_0F_1 -ATP synthase. *J Biochem* 149: 655-664.
8. Mitchell P (2011) Chemiosmotic coupling in oxidative and photosynthetic phosphorylation. *Bio Rev* 41:445-501 (1966). reprinted: *BBA-Bioenergetics* 1807: 1507-1538.
9. Yasuda R, Noji H, Kinosita K, Yoshida M (1998) F_1 -ATPase is a highly efficient molecular motor that rotates with discrete 120° steps. *Journal of Bioenergetics and Biomembranes* 93: 1117-1124.
10. Oster G, Wang H (2000) Energy transduction in the F_1 motor of ATP synthase. *Nature* 32: 459-469.
11. Kinosita K, HNoji, KAdachi, Yasuda R (2000) A rotary molecular motor that can work at near 100% efficiency. *Phil Trans R Soc B* 355: 473-489.
12. Toyabe S, Watanabe-Nakayama T, Okamoto T, Kudo S, Muneyuki E (2011) Thermodynamic efficiency and mechanochemical coupling of F_1 -ATPase. *Proc Natl Acad Sci USA* 108: 17951-17956.
13. Mukherjee S, Warshel A (2011) Electrostatic origin of the mechanochemical rotary mechanism and the catalytic dwell of F_1 -ATPase. *Proc Natl Acad Sci USA* 108: 20550-20555.

14. Mukherjee S, Warshel A (2012) Realistic simulations of the coupling between the protomotive force and the mechanical rotation of the F_0 -ATPase. *Proc Natl Acad Sci USA* 109: 14876-14881.
15. Adachi K, Oiwa K, Nishizaka T, Furuike S, Noji H, et al. (2007) Coupling of rotation and catalysis in F_1 -ATPase revealed by single-molecule imaging and manipulation. *Cell* 130: 309-321.
16. Davies KM, Anselmi C, Wittig I, Faraldo-Gómez JD, Kühlbrandt W (2012) Structure of the yeast F_1F_0 -ATP synthase dimer and its role in shaping the mitochondrial cristae. *Proc Natl Acad Sci USA* 109: 13602-13607.
17. Bouvrais H, Cornelius F, Ipsen JH, Mouritsen OG (2012) Intrinsic reaction-cycle time scale of Na^+, K^+ -ATPase manifests itself in the lipid-protein interactions of nonequilibrium membranes. *Proc Natl Acad Sci USA* 109: 18442-18446.
18. Xing J, Wang H, von Ballmoos C, Dimroth P, Oster G (2004) Torque generation by the F_o motor of the Sodium ATPase. *Biophys J* 87: 2148-2163.
19. Diez M, Zimmermann B, Börsch M, König M, Schweinberger E, et al. (2004) Proton-powered subunit rotation in single membrane-bound F_0F_1 -ATP synthase. *Nature Structural & Molecular Biology* 11: 135-141.
20. Berry RM (2005) ATP synthesis: The world's smallest wind-up toy. *Current Biology* 15: R386.
21. Sielaff H, Rennekamp H, Wächter A, Xie H, Hilbers F, et al. (2008) Domain compliance and elastic power transmission in rotary F_0F_1 -ATP. *Proc Natl Acad Sci USA* 105: 17760-17765.
22. Junge W, Sielaff H, Engelbrecht S (2009) Torque generation and elastic power transmission in the rotary F_0F_1 -ATPase. *Nature* 459: 364-370.
23. Hayashi K, Ueno H, Iino R, Noji H (2010) Fluctuation theorem applied to F_1 -ATPase. *Phys Rev Lett* 104: 218103.
24. Toyabe S, Okamoto T, Watanabe-Nakayama T, Taketani H, Kudo S, et al. (2010) Nonequilibrium energetics of a single F_1 -ATPase molecule. *Phys Rev Lett* 104: 198103.
25. Shimo-Kon R, Muneyuki E, Sakai H, Adachi K, Yoshida M, et al. (2010) Chemo-mechanical coupling in F_1 -ATPase revealed by catalytic site occupancy during catalysis. *Biophys J* 98: 1227-1236.

26. Little MA, Steel BC, Bai F, Sowa Y, Bilyard T, et al. (2011) Steps and bumps: Precision extraction of discrete states of molecular machines. *Biophys J* 101: 477-485.
27. Goldstein BN, Aksirov AM, Zakrjevskaya DT (2011) A model of stepping kinetics for rotary enzymes. application to the F_1 -ATPase. *BioSystems* 104: 9-13.
28. Kohori A, Chiwata R, Hossain MD, Furuike S, Shiroguchi K, et al. (2011) Torque generation in F_1 -ATPase devoid of the entire amino-terminal helix of the rotor that fills half of the stator orifice. *Biophys J* 101: 188-195.
29. Sugawa M, Okada KA, Masaike T, Nishizaka T (2011) A change in the radius of rotation of F_1 -ATPase indicates a tilting motion of the central shaft. *Biophys J* 101: 2201-2206.
30. Iino R, Noji H (2012) Rotary catalysis of the stator ring of F_1 -ATPase. *Biochimica et Biophysica Acta* 1817: 1732-1739.
31. Tanigawara M, Tabata KV, Ito Y, Ito J, Watanabe R, et al. (2012) Role of the delseed loop in torque transmission of F_1 -ATPase. *Biophys J* 103: 970-978.
32. Okazaki K, Hummer G (2013) Phosphate release coupled to rotary motion of F_1 -ATPase. *Proc Natl Acad Sci USA* .
33. Choua T (1999) Kinetics and thermodynamics across single-file pores: Solute permeability and rectified osmosis. *The Journal of Chemical Physics* 110: 606-615.
34. Berezhkovskii AM, Pustovoi MA, Bezrukov SM (2002) Channel-facilitated membrane transport: Transit probability and interaction with the channel. *The Journal of Chemical Physics* 116: 9952-9956.
35. Berezhkovskii AM, Pustovoi MA, Bezrukov SM (2003) Channel-facilitated membrane transport: Average lifetimes in the channel. *The Journal of Chemical Physics* 119: 3943-3951.
36. Berezhkovskii AM, Bezrukov SM (2005) Channel-facilitated membrane transport: Constructive role of particle attraction to the channel pore. *Chemical Physics* 319: 342-349.
37. Berezhkovskii AM, Bezrukov SM (2005) Optimizing transport of metabolites through large channels: Molecular sieves with and without binding. *Biophysical Journal: Biophysical Letters* 88: L17-L19.

38. Bezrukov SM, Berezhkovskii AM, Szabo A (2007) Diffusion model of solute dynamics in a membrane channel: Mapping onto the two-site model and optimizing the flux. *The Journal of Chemical Physics* 127: 115101.
39. Kolomeisky AB (2007) Channel-facilitated molecular transport across membranes: Attraction, repulsion, and asymmetry. *Phys Rev Lett* 98: 048105.
40. Kolomeisky AB, Kotsev S (2008) Effect of interactions on molecular fluxes and fluctuations in the transport across membrane channels. *The Journal of Chemical Physics* 128: 085101.
41. Zilman A (2009) Effects of multiple occupancy and interparticle interactions on selective transport through narrow channels: Theory versus experiment. *Biophysical Journal* 96: 1235-1248.
42. Stock D, Namba K, Lee LK (2012) Nanorotors and self-assembling macromolecular machines: The torque ring of the bacterial flagellar motor. *Current Opinion in Biotechnology* 23: 545-554.
43. Berg HC (2003) The rotary motor of bacterial flagella. *Annu Rev Biochem* 72: 19-54.
44. Thomas DR, Francis NR, Xu C, DeRosier DJ (2006) The three-dimensional structure of the flagellar rotor from a clockwise-locked mutant of salmonella enterica serovar typhimurium. *J Bacteriol* 188: 7039-7048.
45. Meacci G, Tu Y (2009) Dynamics of the bacterial flagellar motor with multiple stators. *Proc Natl Acad Sci USA* 106: 3746.
46. Bai F, Minamino T, Wu Z, Namba K, Xing J (2012) Coupling between switching regulation and torque generation in bacterial flagellar motor. *Phys Rev Lett* 108: 178105.
47. Ryu WS, Berry RM, Berg HC (2000) Torque-generating units of the flagellar motor of *escherichia coli* have a high duty ratio. *Nature* 403: 444.
48. Chen X, Berg HC (2000) Torque-speed relationship of the flagellar rotary motor of *escherichia coli*. *Biophys J* 78: 1036-1041.
49. Gabel C, Berg HC (2003) The speed of the flagellar rotary motor of *escherichia coli* varies linearly with protonmotive force. *Proc Natl Acad Sci USA* 100: 8748-8751.

50. Sowa Y, Hotta H, Homma M, Ishijima A (2003) Torque-speed relationship of the Na^+ -driven flagellar motor of *vibrio alginolyticus*. J Mol Biol 327: 1043-1051.
51. Asai Y, Yakushi T, Kawagishi I, Homma M (2003) Ion-coupling determinants of Na^+ -driven and h^+ -driven flagellar motors. J Mol Biol 327: 453-463.
52. Yuan J, Berg HC (2008) Resurrection of the flagellar rotary motor near zero load. Proc Natl Acad Sci USA 105: 1182-1185.
53. Inoue Y, Lo CJ, Fukuoka H, Takahashi H, Sowa Y, et al. (2008) Torque-speed relationships of Na^+ -driven chimeric flagellar motors in *escherichia coli*. J Mol Biol 376: 1251-1259.
54. Nakamura S, Kami-ike N, Yokota JP, Minamino K, Namba K (2009) Effect of intracellular pH on the torque-speed relationship of bacterial proton-driven flagellar motor. J Mol Biol 386: 332-338.
55. Yuan J, Fahrner KA, Turner L, Berg HC (2010) Asymmetry in the clockwise and counterclockwise rotation of the bacterial flagellar motor. Proc Natl Acad Sci USA 107: 12846-12849.
56. Schmitt R (2003) Helix rotation model of the flagellar rotary motor. Biophys J 85: 843-852.
57. Xing J, Bai F, Berry R, Oster G (2006) Torque-speed relationship of the bacterial flagellar motor. Proc Natl Acad Sci USA 103: 1260-1265.
58. Mora T, Yu H, Wingreen NS (2009) Modeling torque versus speed, shot noise, and rotational diffusion of the bacterial flagellar motor. Phys Rev Lett 103: 248102.
59. Bai F, Lo CJ, Berry RM, Xing J (2009) Model studies of the dynamics of bacterial flagellar motors. Biophys J 96: 3154-3167.
60. Lo CJ, Sowa Y, Pilizota T, Berry RM (2013) Mechanism and kinetics of a sodium-driven bacterial flagellar motor. Proc Natl Acad Sci USA .
61. Fisher ME, Kolomeisky AB (2001) Simple mechanochemistry describes the dynamics of kinesin molecules. Proc Natl Acad Sci USA 98: 7748-7753.
62. Kolomeisky AB, Fisher ME (2007) Molecular motors: A theorist's perspective. Ann Rev Phys Chem 58: 675-695.

63. Fisher ME, Kolomeisky AB (1999) Molecular motors and the forces they exert. *Physica A* 274: 241-266.
64. Toyabea S, Watanabe-Nakayamab T, Okamotoa T, Kudoc S, Muneyukia E (2011) Thermodynamic efficiency and mechanochemical coupling of f_1 -ATPase. *Proc Natl Acad Sci USA* 108: 17951-17956.
65. Meng X, Yu M, Zhang Y (2013) The load dependence of the physical properties of a molecular motor. *J Phys: Condens Matter* 25: 374102.
66. Derrida B (1983) Velocity and diffusion constant of a periodic one-dimensional hopping model. *J Stat Phys* 31: 433-450.
67. Zhang Y (2009) Derivation of diffusion coefficient of a brownian particle in tilted periodic potential from the coordinate moments. *Physics Letters A* 373: 2629-2633.
68. Visscher K, Schnitzer MJ, Block SM (1999) Single kinesin molecules studied with a molecular force clamp. *Nature* 400: 184-189.
69. Zhang Y (2009) The efficiency of molecular motors. *J Stat Phys* 134: 669-679.
70. Zhang Y (2009) A general two-cycle network model of molecular motors. *Physica A* 383: 3465-3474.
71. Zhang Y (2011) Growth and shortening of microtubules: A two-state model approach. *J Biol Chem* 286: 39439-39449.
72. Klumpp S, Lipowsky R (2005) Cooperative cargo transport by several molecular motors. *Proc Natl Acad Sci USA* 102: 17284-17289.
73. Müller MJ, Klumpp S, Lipowsky R (2008) Tug-of-war as a cooperative mechanism for bidirectional cargo transport by molecular motors. *Proc Natl Acad Sci USA* 105: 4609-4614.
74. Zhang Y (2009) Properties of tug-of-war model for cargo transport by molecular motors. *Phys Rev E* 79: 061918.

Tables

Table 1. The parameter values of the two-state model used in this study, which are obtained by fitting the rotation speed formulation listed in Eq. (6) to the experimental data measured in [60]. The total number of free parameter is 10, since ϵ_4, ϵ'_4 can be obtained by the normalization condition, $\sum_{i=1}^4 \epsilon_i = \sum_{i=1}^4 \epsilon'_i = 1$.

parameter	value (s ⁻¹)	parameter	value	parameter	value
\hat{k}_1^0	1993.2	ϵ_1	0.16	ϵ'_1	0
k_2^0	43.8	ϵ_2	0.54	ϵ'_2	0.76
k_3^0	324.0	ϵ_3	0.3	ϵ'_3	0.08
\hat{k}_4^0	8258.5	ϵ_4	0	ϵ'_4	0.16

Figure Legends

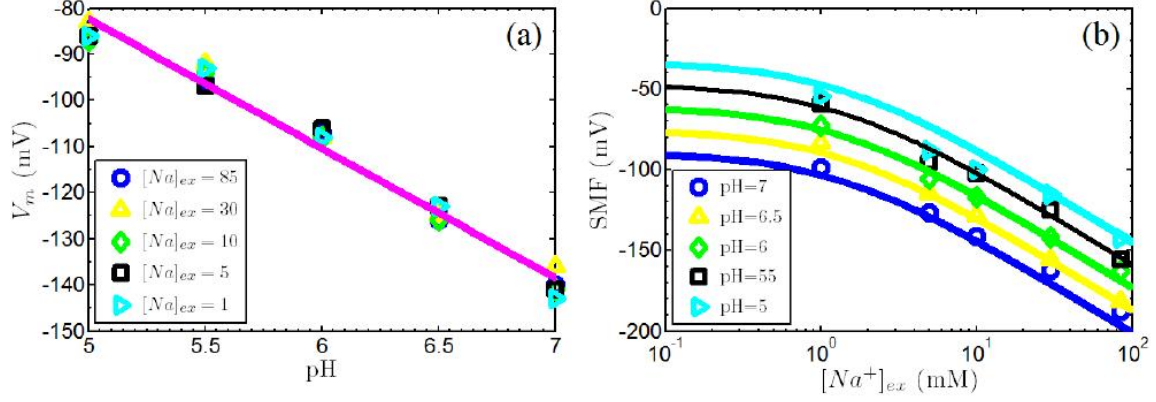


Figure 1. (a) The relationship between pH value and membrane voltage V_m , which is used to get electrical energy $U = qV_m$, can be well approximated by $V_m = -28.04\text{pH} + 57.88$, see Eq. (1). (b) The sodium-motive force (SMF) can be approximately obtained by $\text{SMF} = V_m + k_B T / q \ln[9.013 / (1.318 + [Na]_{ex})]$, which means the internal sodium concentration $[Na]_{in}$ can be obtained by the external sodium concentration $[Na]_{ex}$, $[Na]_{in} = 9.013[Na]_{ex} / (1.318 + [Na]_{ex})$, see Eq. (7). In this figure, all the data are from [60].

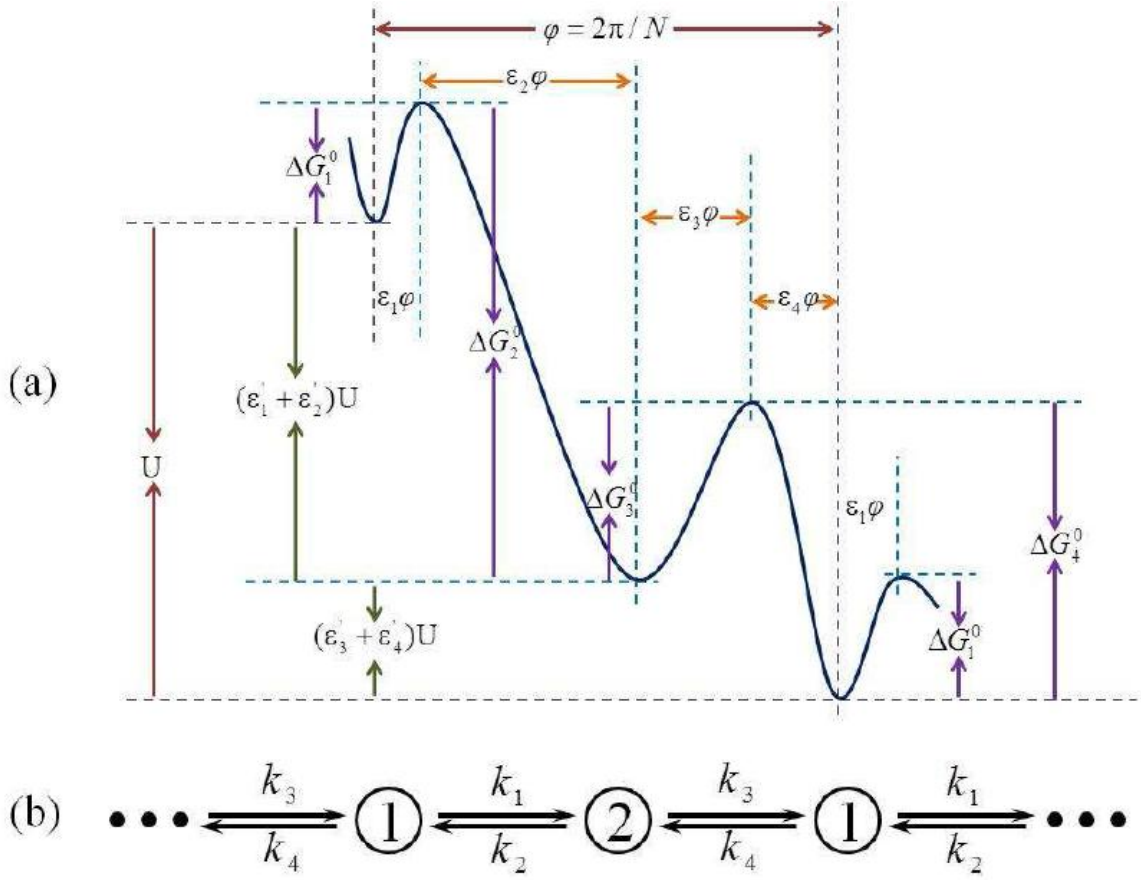


Figure 2. Schematic depiction of the two-state model for stator rotation. **(a)** The stator is assumed to move in one tilted periodic potential $G(\theta)$ with period $\varphi = 2\pi/N$. Where $N = 37$ is the number of ions which cross the membrane in each revolution of bacterial flagellar motor [60]. Under no external torque, the energy difference in one period is equal to the electrical energy U released by one ion crossing membrane. The *distribution factors* ϵ_i and ϵ'_i satisfy the normalization condition $\sum_{i=1}^4 \epsilon_i = \sum_{i=1}^4 \epsilon'_i = 1$, and for simplicity they are assumed to be independent of external torque Γ and the electrical energy U [65]. With the increase of external torque, the forward rotation barriers (in this figure $\Delta G_1^0, \Delta G_3^0$ are the energy barriers when external torque vanishes) will be increased, while the backward rotation barriers (similarly, $\Delta G_2^0, \Delta G_4^0$ are the backward energy barriers when external torque vanishes) will be decreased. Consequently, the degree of the potential tilt will be decreased. The two states of the stator are corresponding to the two minima of the potential. $\epsilon_i \varphi$ is the mechanical angle between stable state of the stator and its rotation energy barrier. The rotation speed of stator increases with electrical energy U but decreases with external torque Γ . **(b)** Mathematically, the stator rotation in the periodic tilted potential depicted in **(a)** can be described by one Markov process with two biochemical state, denoted by state **1** and state **2** respectively. In which one forward biochemical cycle $1 \xrightarrow{k_1} 2 \xrightarrow{k_3} 1$ is coupled with one forward mechanical rotation of angle φ . The transition rates k_i depend on electrical energy U , external torque Γ , ion concentration and pH value, which are given by formulations in (5).

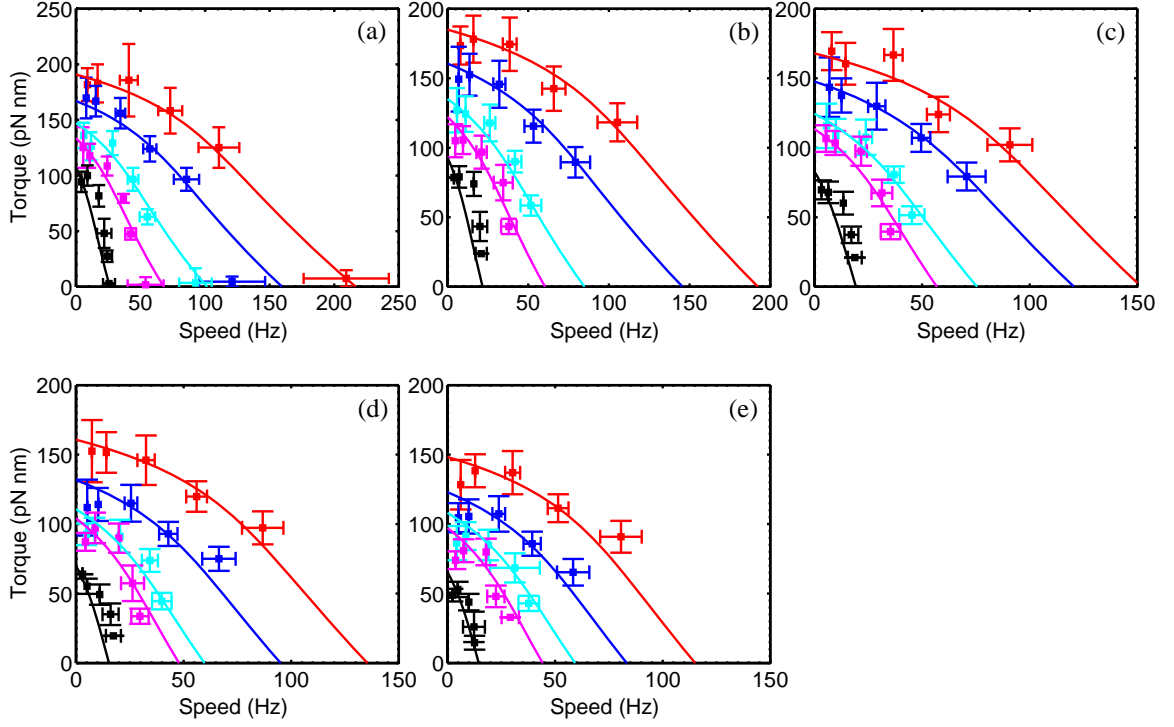


Figure 3. Torque-speed relationships of one-stator BFM for (a) pH=7, (b) pH=6.5, (c) pH=6, (d) pH=5.5, and (e) pH=5. From right to left, the lines are for external sodium concentration $[\text{Na}]_{ex}=85$ mM, 30 mM, 10mM, 5 mM, and 1 mM respectively. The experimental data are from [60], and the lines are obtained from the two-state model [see Eq. (6)] with model parameter values listed in Table 1.

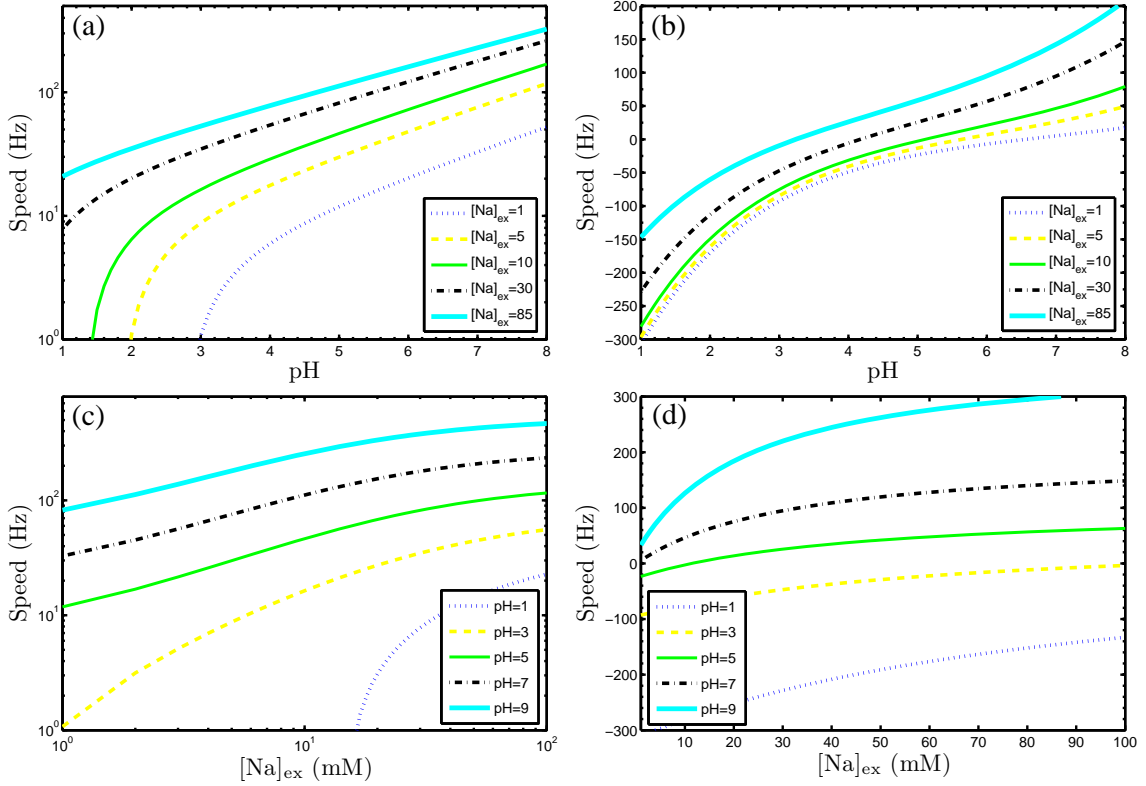


Figure 4. The rotation speed V of one-stator BFM increases with pH value and external sodium concentration $[Na]_{ex}$. For high pH value, speed V increases almost experimentally with pH. In (a, c), the torque $\Gamma = 0$, and in (b, d), the torque $\Gamma = 100$ pN·nm. For high values of Γ and low values of pH and sodium concentration $[Na]_{ex}$, the stator will rotate reversely.

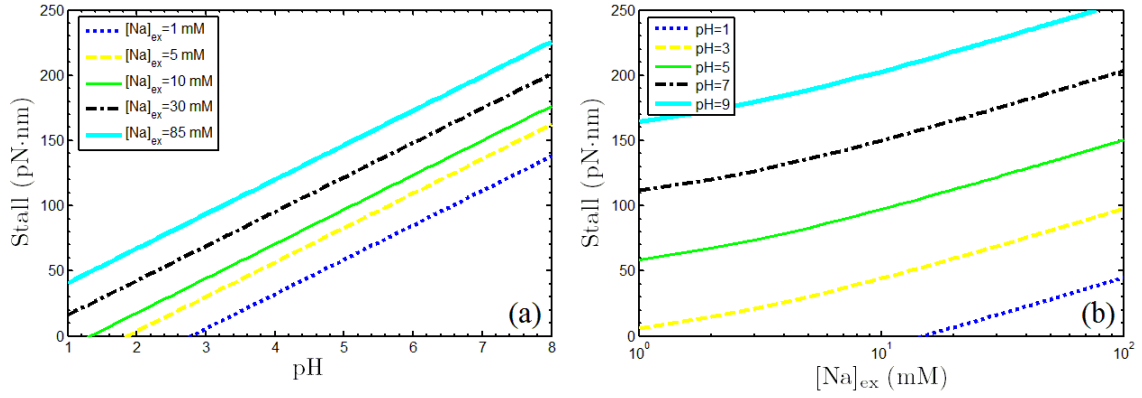


Figure 5. The *stall torque* Γ_s , i.e. the torque under which the rotation speed of BFM vanishes, increases with pH value (linearly) and external sodium concentration $[Na]_{ex}$, see the formulation in Eq. (7) [Note, the figures are obtained directly by $V(\Gamma_s) = 0$, see the corresponding formulation of speed V in Eq. (6)].

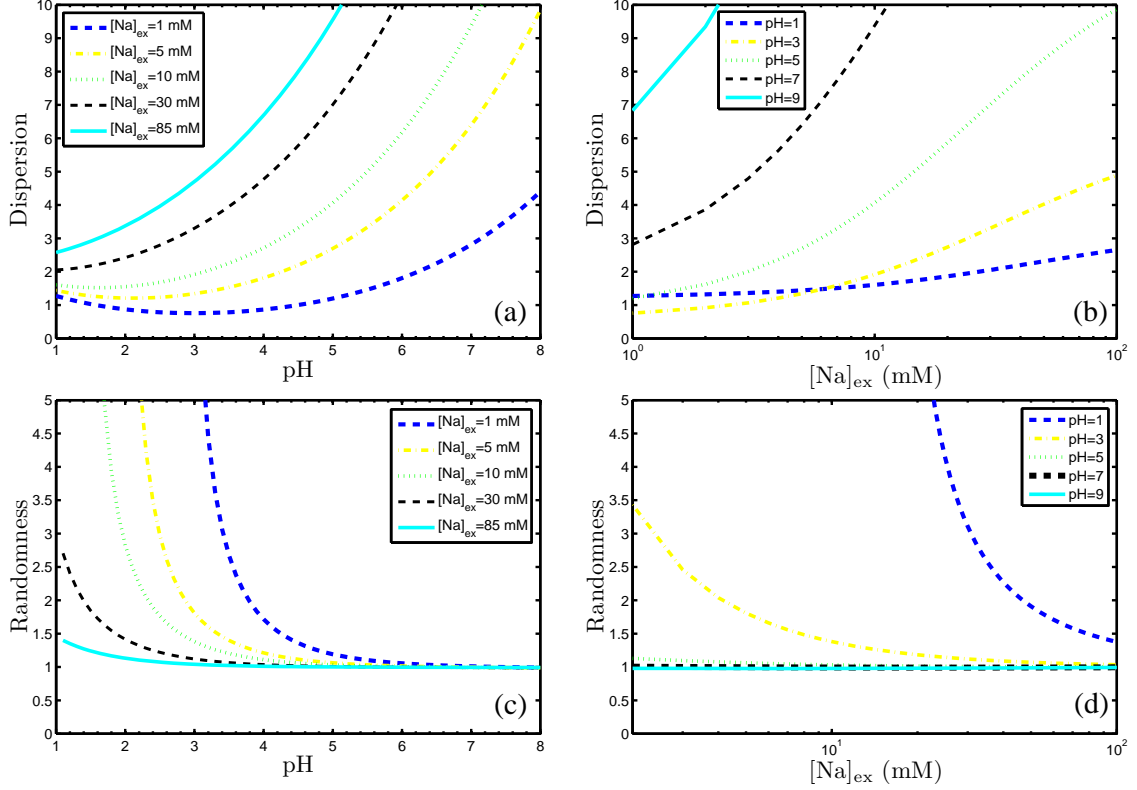


Figure 6. The dispersion D and randomness r of BFM rotation. **(a)** For high sodium concentration, dispersion D increases with pH value (**note**, for low sodium concentration and low pH values, the rotation speed V is negative, see Fig. 4); **(b)** Dispersion D increases with sodium concentration $[Na]_{ex}$. With the increase of pH value and sodium concentration, randomness $r = 2D/V\varphi$ decreases monotonically to 1 **(c, d)**. Which means that, for high pH value and $[Na]_{ex}$, the rotation of BFM is just one Poisson process. In all figures, the external torque is zero.

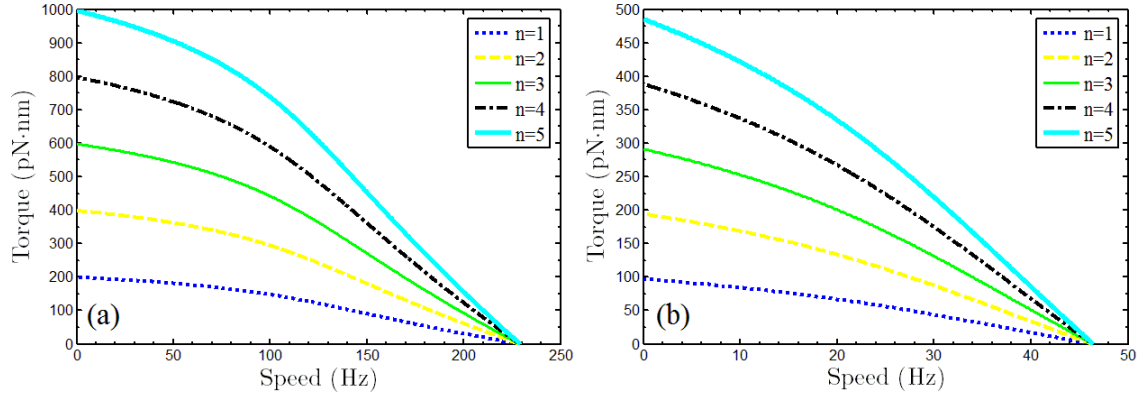


Figure 7. Torque-speed relationships if the external torque Γ is shared equally by n stators for $n = 1, 2, 3, 4, 5$ respectively. **(a)** pH=7 and $[Na]_{ex} = 85$ mM, **(b)** pH=5 and $[Na]_{ex} = 10$ mM. The figures are similar as the ones obtained in [45, 47].

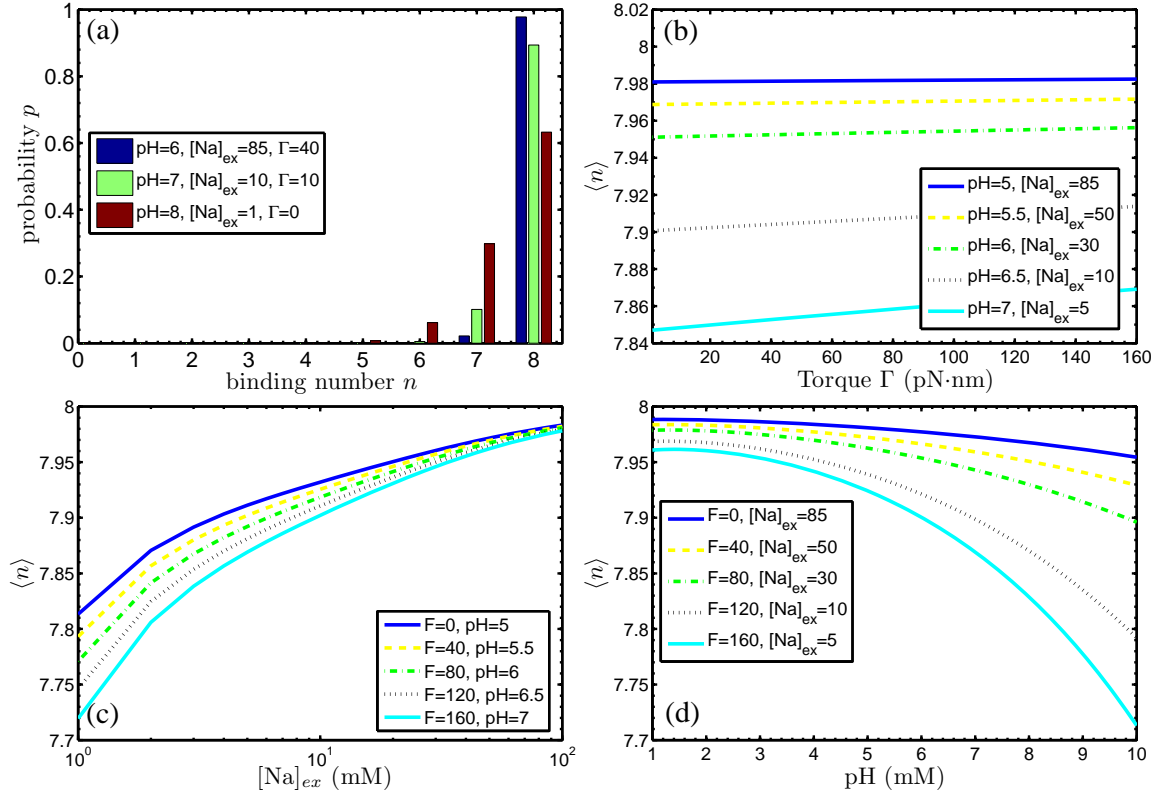


Figure 8. (a) Probability of stator number binding to BFM rotor. In most cases, almost all stators are bound to BFM rotor, i.e. the duty ratio of stator is high [47]. (b) With the increase of external torque Γ , the mean binding number $\langle n \rangle$ of stator will be increased. Meanwhile, the mean binding number $\langle n \rangle$ increases with sodium concentration $[\text{Na}]_{\text{ex}}$ (c), but decreases with pH value (d). In all the figures, the total number of stator is assumed to be $M = 8$.

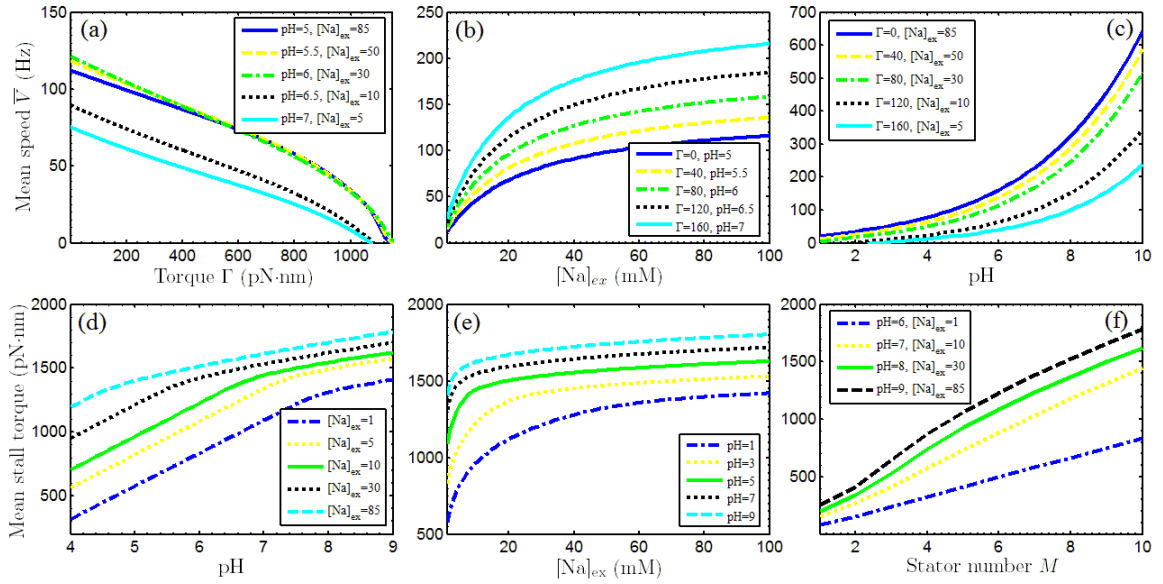


Figure 9. The mean rotation speed \bar{V} and mean stall torque $\bar{\Gamma}_s$ of BFM with total stator number $M = 8$. Here \bar{V} is obtained by $\bar{V} = \sum_{n=1}^M p_n V_n$, in which p_n is the probability that BFM rotor is bound by n stators, and V_n is the rotation speed of BFM if the external torque is shared by n stators. The mean stall torque $\bar{\Gamma}_s$ is obtained by $\bar{V}(\bar{\Gamma}_s) = 0$. Similar as the one single stator cases, the mean rotation speed \bar{V} decreases with external torque Γ (a), and increases with external sodium concentration $[\text{Na}]_{\text{ex}}$ and pH value (b, c). Meanwhile, the mean stall torque $\bar{\Gamma}_s$ increases with $[\text{Na}]_{\text{ex}}$, pH value and total stator number M (d, e, f).